Self-Assembling Peptide Inspired by a Barnacle Underwater Adhesive Protein

Masahiro Nakano,[†] Jian-Ren Shen,[‡] and Kei Kamino*[,†]

Marine Biotechnology Institute, 3-75-1 Heita, Kamaishi, Iwate 026-0001, Japan, and The Graduate School of Natural Science and Technology, Okayama University, Tsushima-Naka 3-1-1, Okayama 700-8530, Japan

Received December 23, 2006; Revised Manuscript Received March 12, 2007

An underwater bioadhesive generally comprises a multiprotein complex that provides a molecular basis for self-assembly. We report here a new class of self-assembling peptide inspired by a 20 kDa barnacle cement protein. Studies on the chemically synthesized 24-residue peptide have revealed that (1) it underwent irreversible self-assembly upon the addition of salt, (2) the self-assembly was started at a salt concentration close to that of seawater with noncovalent intermolecular interactions, (3) the self-assembled material resembled a macroscopic membrane of interwoven nanofilaments, (4) incubation in an alkaline pH range formed the intramolecular disulfide bond of a peptide molecule, thus triggering a conformation change of the molecule, and (5) conformational change of the building block promoted the formation of a nanofiber, resulting in the display of a three-dimensional meshlike mesoscopic structure with defined pores having a diameter of approximately 200 nm. The peptide is likely to provide a suitable basis for further development of peptide-based materials.

Introduction

Studies of the bioadhesive molecular systems in diverse aquatic sessile organisms[1,2] could benefit the design of new biomaterials and biomimetics that may lead to significant advances in nanobiotechnology. The barnacle, a unique sessile crustacean, attaches to diverse foreign material surfaces by an extracellular underwater adhesive complex, historically called cement. This cement[3] is a multiprotein complex whose subunits are distinct from each other and have no similarity to the other well-studied model system, mussel holdfast proteins, in the sequences and post-translational modifications.[4,5] Underwater attachment involves a number of functions such as displacement of the bound-water layer, spreading, coupling, curing, cleaning of biofilms, and protection from microbial degradations that are well-coordinated, each with crucial timing. These functions[6] also include control of the homo- and hetero-self-assembly of underwater adhesive proteins so that the proteins would qualify for molecular interaction.

A peptide-based material is the leading example to combine a biological molecule with material science. It provides several advantages, including molecular diversity, simple design from a biological aspect, and ease of integrating a biological motif. Interest in this material has spread across diverse research areas including nanotechnology[7] and biomaterial development in regenerative medicine and tissue engineering.[8,9] Molecular self-assembly in a noncovalent fashion is one of the most attractive molecular fabrication methods for a peptide-based material. Some of these have originated from part of a biological molecule,[10−12] and some have been rationally designed,[13] while others have used a combination of molecular engineering techniques[14] or a combination of chemical methods.[15−19] Further studies on biological molecular self-assembling systems will lead to the discovery and advance of new artificially produced materials. Peptide mimetic research on mussel foot protein[20, 21] has almost completely relied on the versatile modified amino acid, 3,4-dihydroxyphenylalanine, for its capabilities of cross-linking and adsorption. The present study raises further potential for a biotic underwater adhesive of simple peptide design based on protein−protein interaction in a noncovalent fashion.

Megabalanus rosa cement protein 20 kDa (Mrcp-20k)[22] is a barnacle cement protein that is characterized by the abundance of charged amino acids and cysteine. The alignment of cysteines indicates that the primary structure has six repetitive sequences, although many of the amino acids among them are not conserved, except for cysteines and a few others. The abundant charged amino acids are likely to play a functional role, because all of the cysteines that form intramolecular disulfide bonds are essential for conformational stability. The isolation of a homologous gene from another species, *Balanus albicostatus*, has also revealed the protein to be rich in charged amino acids and cysteine, with the primary structure organized into four repetitive sequences (unpublished data). This different repetition number in the two cp-20k's might suggest that a repetition is the minimum structural and functional unit, which prompted us to study the properties of peptides designed from the repetitive sequence in cp-20k.

We report here that peptides derived from the repetitive sequences in Mrcp-20k showed salt-dependent self-assembly into a macroscopic membrane. We propose from the results obtained that this underwater bioadhesive represents a good model for designing and fabricating new classes of peptide-based self-assembling materials.

Materials and Methods

Preparation of the Peptides. The peptides designed in this study originated from repetitive units in the primary structure of Mrcp-20k.[22] cMr20-S5 corresponds to the fifth single repetitive sequence in Mrcp-20k, Ac-SKLPCNDEHPCYRKEGGVVSCDCK-NH_2. All of the Cys

* Author to whom correspondence should be addressed. E-mail: kei.kamino@mbio.jp.

[†] Marine Biotechnology Institute.

[‡] Okayama University.

10.1021/bm0612236 CCC: $37.00
Published on Web 05/23/2007

residues in cMr20-S5 have been replaced by Ser in cMr20-S5(Ser). cMr20-S6 corresponds to the sixth single repetitive unit with the following sequence: Ac-KTITCNEDHPCYHSYEEDGVTKSDCDCE-NH_2. RAD16-I and the human parathyroid hormone fragment (PTH) were also prepared for respective use as positive and negative controls. RAD16-I is a typical peptide that has been found to self-assemble upon the addition of salt.[23] PTH (residues 13−34)[24] has roughly similar amino acid length and charged amino acid content to the peptides designed in this study. The peptides were chemically synthesized (Peptide Institute, Japan) with an ABI 430A automated peptide synthesizer (Applied Biosystems, Foster City, CA), using standard Boc chemistry. The α-amino group at the N-terminus and α-carboxyl group at the C-terminus of each peptide were respectively N-acetylated (Ac-) and C-amidated (−NH_2). The peptide was cleaved from the support, purified by reverse-phase HPLC in a Zorbax 300SB-C18 column (4.6 mm × 150 mm; Agilent Technologies, Palo Alto, CA), freeze-dried, and stored at −20 °C. The Cys residues in each peptide were introduced as cysteine (with a free sulfhydryl group) and maintained under acidic conditions during the purification process. The purity of the peptide was more than 95%. The molecular mass of peptide was confirmed by the electrospray ionization mass spectrometry (ESI-MS) with a HP1100 series LC/MS-detector instrument (Agilent Technologies, CA). The peptide was dissolved in ultrapure water (Milli-Q system, Millipore, Bedford, MA) or 10 mM of a sodium phosphate buffer at pH 6 in a polypropylene tube immediately before use for the self-assembly process. The peptide was dissolved in a 10 mM sodium phosphate buffer at pH 8 and then stood overnight at ambient temperature for the alkaline pretreatment. A 10 mM ammonium acetate buffer (pH 8) was exceptionally used only in the alkaline pretreatment for the ESI-MS analysis described below.

Evaluation of the Chemical Form of the Cys Residues. An alkylation treatment was carried out to detect the free thiol group. Approximately 2 μM peptide in 7 M guanidine hydrochloride/1.5 M Tris (pH 8)/20 mM EDTA was treated with the alkylating agent, 0.8 mM of mono-iodoacetic acid, for 2 h in the dark at ambient temperature, and was then desalted by reverse-phase HPLC. Alkylation of the peptide was confirmed by matrix-assisted laser desorption ionization time-of-flight (MALDI-TOF) MS. MALDI-TOF MS was measured by using a Voyager-DE instrument (Perkin-Elmer, Boston, MA). Saturated sinapinic acid in 0.1% trifluoroacetic acid/30% acetonitrile was used as the MALDI-TOF MS matrix. A Sequazyme Peptide Mass Standards kit (mixture 3; PE Biosystems, Foster City, CA) was used as a calibration standard. ESI-MS was measured by an LCQ-Advantage instrument (Thermo Electron, Waltham, MA). The peptide solution (0.05 mg/mL) was diluted by 0.1% formic acid/90% acetonitrile with a dilution factor of 10 before injection.

Evaluation of the Self-Assembly Process. Self-assembly was initiated by mixing the peptide solution with or without the alkaline pretreatment with a salt solution to a final concentration of 1 M NaCl in a polypropylene tube and allowed to stand for 10 min at ambient temperature. The salt solutions used were aqueous NaCl or NaCl dissolved in phosphate-buffered saline (PBS; 137 mM NaCl/2.7 mM KCl/8.1 mM Na_2HPO_4/1.5 mM KH_2PO_4), each being 0.22-μm-filtered before use. The hydrodynamic radius of self-assembled particles was measured with dynamic light scattering (DLS) using a DynaPro instrument (Protein Solutions, Charlottesville, VA). The dilution factor of a sample was always 2, the sample mixture being centrifuged at 15 000 rpm for 5 min and the resulting supernatant used for the analysis within 5 min. Each set of data was obtained by integrating the results of 20−30 scans. Two types of reduction treatment were used for the DLS measurement: (1) The peptide solution was first reduced by more than 4 times the molar ratio of dithiothreitol (DTT) at ambient temperature for 5 min, mixed with the salt solution, and then measured. (2) The peptide that had undergone self-assembly under the increasing NaCl concentrations was first measured. DTT was subsequently added to the peptide solution, the mixture then being incubated and measured again. Treatment with metal chelating agent was carried out as follows. The peptide that had undergone self-assembly by the addition of 1 M NaCl was dialyzed against water twice for 2.5 h, mixed with EDTA solution (pH 8) to a final concentration of 0.1 M, incubated at ambient temperature for 24 h, and then subjected to DLS measurement.

The evaluation by gel filtration chromatography (GFC) was carried out as follows. The peptide solution with or without the alkaline pretreatment was diluted with 0.1% trifluoroacetic acid/45% acetonitrile by a dilution factor of 20 (final 0.25 mg/mL), centrifuged at 15 000 rpm for 5 min, and subjected to GFC in a TSK gel $G2000SW_{XL}$ column (7.8 mm × 30 cm; Tosoh, Japan). The molecular weight was calculated by a standard curve using molecular markers (oxytocin, M_r 1007 Da; bombesin, M_r 1619 Da; aprotinin, M_r 6500 Da; myoglobin, M_r 17 800 Da).

Visualization by Atomic Force Microscopy and Scanning Electron Microscopy. The peptide self-assembly was first desalted by dialysis before the atomic force microscopy (AFM) analysis. Dialysis was performed against a sufficient amount of ultrapure water or a buffer solution at 4 °C. A 10 μL aliquot of the resulting dialysate was placed on the newly peeled surface of a mica wafer and briefly dried at ambient temperature. An AFM image in the tapping mode was captured by a Nanoscope IIIa controller (Digital Instruments, Santa Barbara, CA) and multimode AFM instrument (Olympus, Japan), using a silicon probe with a cantilever length of 160 μm and a spring constant of 42 N/m. Images with a scanning range of 0.5−10 μm were taken at a scanning rate range of 0.6−1 Hz with 256 lines per image. The value of the width of a nanofilament or -fiber was taken from the mean value of 30 random samples.

For the scanning electron microscopy (SEM) observation, self-assembly was performed on the surface of mica attached on the inner bottom of the dish before rinsing by gently adding 100 volumes of pure water to the dish. The addition of excess water made the self-assembled peptide peel off and thereby easier to handle. The self-assembly was fixed for 30 min in a 5% glutaraldehyde/0.1 M cacodylate buffer at pH 7.2 and 4 °C, before being sequentially dehydrated with 10%, 20%, 50%, 70%, 90%, and 100% ethanol for 5 min each. The sample was subjected to critical point drying, before being coated with platinum particles, mounted on a grid, and examined by an S2500 scanning electron microscope (Hitachi, Japan).

Evaluation of the Secondary Structure of the Peptide. Circular dichroism (CD) spectra of the peptide solutions were measured with a J725 spectropolarimeter (Jasco, Japan). The salt dependence of the secondary structure of the peptide was evaluated by diluting the peptide solution with 10 mM of a sodium phosphate buffer at pH 6.8 containing 0−1.0 M NaCl to a dilution factor of 20. The solution was incubated for 10 min at room temperature and then dialyzed against 10 mM sodium phosphate buffer at pH 6.8 before the CD spectrum was measured. The pH dependence of the secondary structure of the peptide was evaluated in a similar manner, except that the peptide solution was diluted by the buffer solution in a pH range of 2−10, the mixture then being incubated overnight at each corresponding pH value or for 3 h at pH 8 before measurement. The CD spectra were corrected by converting to the mean residual ellipticity to account for different molecular weights and concentrations.

Dominancy of the cross-β structure was evaluated by Congo red staining.[25] A self-assembled peptide prepared in the same way as that for SEM observation was mixed with a Congo red solution to a final concentration of 5 μg/mL, stood for 1 h at room temperature, and observed.

Results

Peptide Preparation. All peptides synthesized in this study were soluble in water. The monomeric form of the cMr20-S5 molecule and chemical form of the Cys residues in the peptide were confirmed using MS and GFC (Table 1). TOF-MS gave the monomeric molecular masses of the peptide with and without the alkaline pretreatment. GFC indicated no larger peptide aggregate in either peptide with or without the alkaline

Table 1. Confirmation of the Monomeric Form of cMr20-S5 and Chemical Form of Cys in the Peptide[a]

	molecular mass (Da)					
	GFC		ESI-MS		MALDI-TOF MS	
	no incubation	O.N. incubation	no incubation	O.N. incubation	no addition of alkylating agent	addition of alkylating agent
cMr20-S5 in water	3745.6	3660.9	2708.7	2708.7	2700.3	2934.1
cMr20-S5 preincubated at pH 8	3703.0	3195.5	2709.0	2705.4	2702.2	2701.9

[a] Theoretical molecular masses of cMr20-S5 are as follows: peptide with all cysteines, 2709.1 Da; that with all cystines, 2705.1 Da; that with alkylation of cysteines, 2941.2 Da. "O.N." denotes overnight.

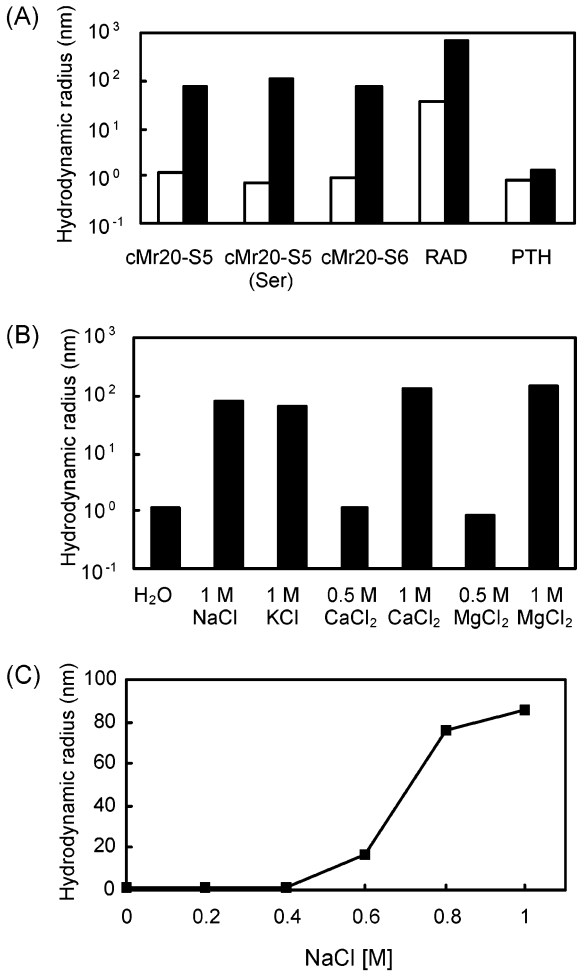

Figure 1. Dynamic light scattering analyses for evaluating peptide self-assembly. (A) The effect of NaCl concentration on the increase in the hydrodynamic radius of each peptide (a final peptide concentration of 5 mg/mL) was evaluated by DLS measurements. DLS was measured in the absence (open bar) or presence (closed bar) of 1 M NaCl. (B) The salt-species dependence in the self-assembly of cMr20-S5 was evaluated. (C) The dose dependence of the NaCl concentration on self-assembly was measured. The peptide, cMr20-S5, was incubated in salt solutions of 0.2−1 M NaCl, and its hydrodynamic radius was measured by DLS.

pretreatment. Although the peptide immediately after dissolving in the alkaline solution gave the same elution time by GFC as that in water, the elution time was slightly longer after the overnight incubation in the alkaline solution. The latter might be due to formation of a compact conformation. ESI-MS measurements further indicated that the peptide in water or immediately after dissolving in the alkaline solution had a monomeric molecular mass with all cysteines (i.e., sulfhydryl form), while it had a monomeric molecular mass with all cystines, (i.e., disulfide bond form) after the overnight alkaline pretreatment. An alkylation test by TOF-MS confirmed that all the Cys residues of the peptide in water had retained a free sulfhydryl group. No alkylation occurred after the alkaline pretreatment, indicating that all of the Cys residues had formed intramolecular disulfide bonds.

Salt-Concentration-Dependent Peptide Self-Assembly. Self-assembly of the peptides was evaluated by DLS measurements. Increasing the NaCl concentration to 1 M resulted in a marked increase in the hydrodynamic radius of both cMr20-S5 and cMr20-S6 by up to approximately 100 nm (Figure 1A). The increment was not affected by metal chelator (EDTA) treatment (data not shown). An evaluation of the salt-species dependence showed that all of the salts tested in this study were effective in inducing self-assembly (Figure 1B). Although a 0.5 M concentration of the divalent cation species did not trigger self-assembly, 1 M of the monovalent cation species did. The involvement of intermolecular disulfide bond formation in the self-assembly of the peptide was evaluated by treating with the reductant, DTT. DLS measurements showed that the DTT treatment had no effect on the self-assembly (data not shown). A peptide in which all four cysteines in cMr20-S5 had been replaced with Ser, named cMr20-S5(Ser), was synthesized to ensure the independence of intermolecular disulfide bond formation in the self-assembly process. DLS measurements revealed that the hydrodynamic radius of cMr20-S5(Ser) was similarly increased by the addition of salt (Figure 1A). The dose dependence of the NaCl concentration in the self-assembly of cMr20-S5 was then evaluated (Figure 1C): Self-assembly was not apparent in less than 0.6 M NaCl, but the peptide was self-assembled above this salt concentration. The DLS data indicated that the self-assemblies were polydispersed. Salt-dependent self-assembly of cMr20-S5 on mica gave a macroscopically distinguishable membrane (approximately 1−10 mm on each side) that could be peeled off as a discrete layer. cMr20-S5(Ser) also formed a similar macroscopic assembly (data not shown).

Visualization of the Microscopic Structures of the Peptide Assemblies. The microscopic structure of cMr20-S5 that had self-assembled in 1 M NaCl/PBS was observed by AFM and SEM. It was indicated that nanofilaments were interwoven to form a membrane (Figures 2A and 2B), called "the standard filament structure" in this study. The filaments had similar widths (83 ± 31 nm) and varied in length (500 nm to several micrometers). Self-assembly was not apparent without the addition of salt (Supporting Information, Figure 1C). AFM imaging and SEM observation of cMr20-S5(Ser) also gave images indistinguishable from those of cMr20-S5 (Supporting Information, Figures 1A and 1B). No noticeable difference was apparent in the images of the self-assembled peptides between the two peptides, cMr20-S5 and cMr20-S6 (data not shown), although cMr20-S6 did not form a macroscopic membrane. Treatment with metal chelating agent (EDTA) did not affect the AFM image of cMr20-S5. The salt-dependent self-assembly of cMr20-S5 with an alkaline preincubation resulted in an individual mesoscopic structure (Figures 2C and 2D). The AFM images showed a "meshlike" structure with a mean pore size

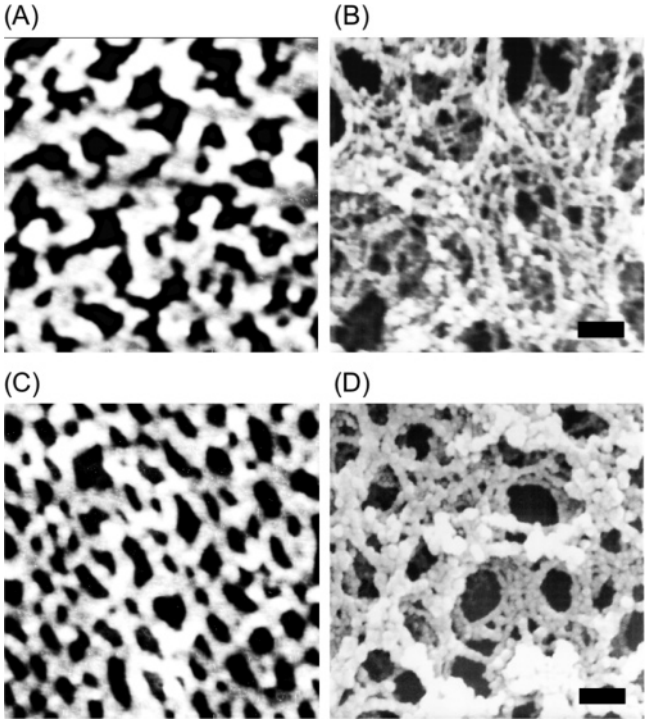

Figure 2. Atomic force microscopy and scanning electron microscopy observations of the self-assembled peptide. Mircroscopic structures of the cMr20-S5 self-assemblies in 1 M NaCl/PBS (A and B) and in 1 M NaCl with alkaline preincubation (C and D). The AFM images (A and C, a square, 3 μm each side) were captured in the tapping mode with a 0.8 Hz scanning rate in air. The self-assemblies were prepared by each process with 100 μM of peptide solution. The SEM images (B and D) were taken with a magnification of $\times$30 000. A higher concentration of the peptide (final concentration of 8 mg/mL) was used to give membraneous self-assembly. Scale bar indicates 0.5 μm in length.

of 161 $\pm$ 68 nm and a meshwork width of 101 $\pm$ 36 nm. SEM indicated the meshwork to be a bundle of nanofilaments, referred to as the fiber. The conditions for the formation of this meshlike structure were investigated and are summarized in Table 2. Briefly, substituting a 10 mM Tris buffer at pH 8 for sodium phosphate buffer had no effect on the formation of the meshlike structure (Table 2, row 5). This image was not apparent in the self-assembly with overnight preincubation in water (row 2) or with overnight preincubation at pH 6 (row 3). The structure was formed by self-assembly with alkaline preincubation and dialysis at pH 6 (row 6), although a 3 h preincubation at pH 8 with dialysis at pH 6 did not give this structure (row 8). Once the meshlike structure had been formed by the self-assembly with alkaline preincubation and dialysis, the structure could be maintained by additional dialysis at pH 6 (row 9). After self-assembly at pH 6, immediate dialysis at pH 8 produced a meshlike structure (row 10). However, additional dialysis at pH 8 after complete desalting by dialysis at pH 6 did not form a meshlike structure (row 11). The cysteine-free peptide, cMr20-S5(Ser), did not form a meshlike structure with the alkaline preincubation (row 13).

Evaluation of the Secondary Structure of the Self-Assembled Peptides. The secondary structure of the self-assembled peptides was examined by CD spectrometry and Congo red staining. The CD spectrum of cMr20-S5 in a sodium phosphate buffer at pH 6.8 showed neither a β-sheet structure nor any defined secondary structure (Figure 3A). The addition of salt at pH 6.8 did not affect the CD spectrum. A partial structural change was observed after cMr20-S5 had been simply preincubated overnight at pH 8−10 (Figure 3B). Sequential

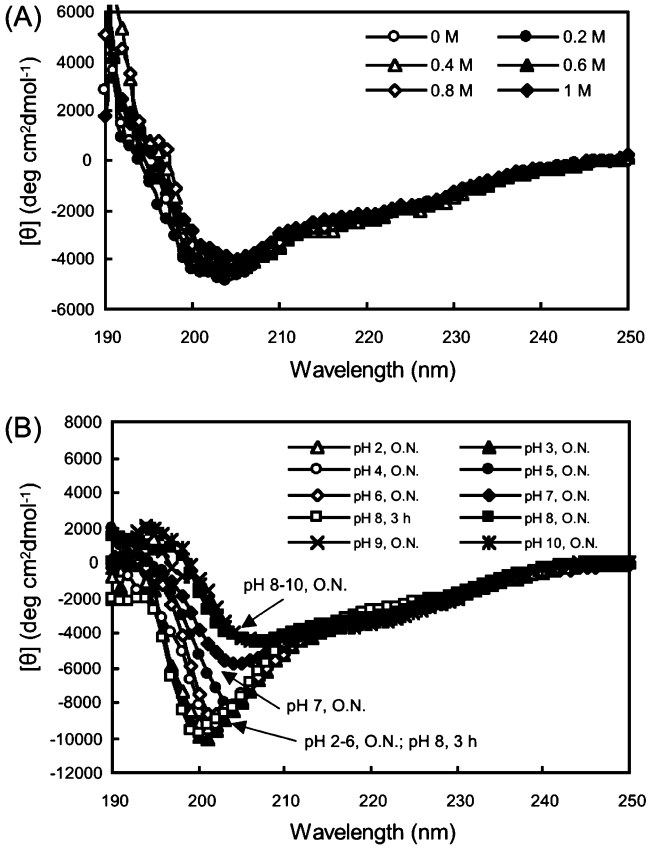

Figure 3. Circular dichroism spectra of cMr20-S5. (A) CD spectra of cMr20-S5 in a salt solution are shown. cMr20-S5 (20 μM) was incubated with 0−1 M NaCl, dialyzed to remove the salt, and subjected to CD spectral measurement. The CD spectra before dialysis were similar to those after dialysis, except for the spectra being affected by salt at shorter wavelengths. (B) The pH dependence of the CD spectra of cMr20-S5 is shown. The procedure used was similar to that for part A, except for the pH range of 2−10 and the omission of NaCl in the overnight incubation. The CD spectrum after 3 h of preincubation at pH 8 was also measured. The buffers used in this experiment were as follows: 10 mM sodium phosphate (pH 2, 3, 6, 7, or 8), 10 mM sodium acetate (pH 4 or 5), and 10 mM sodium borate (pH 9 or 10).

overnight preincubation at pH 6 after overnight preincubation at pH 8 did not affect the CD spectrum, indicating that the change in the CD spectrum at pH 8 was irreversible (data not shown). The CD spectrum with preincubation at pH 8 for 3 h was similar to that with incubation at less than pH 7 (Figure 3B). cMr20-S5(Ser) gave the same CD spectrum in the pH range of 2−10 (data not shown). The Congo red treatment, which preferentially stains a cross-β structure, did not produce any evident staining of macroscopically self-assembled cMr20-S5, while self-assembled RAD-16 was clearly stained.

Discussion

The salt-dependent self-assembly behavior of the peptide designed from a 20 kDa barnacle cement protein was analyzed in the present study, because self-assembly is one of the indispensable functions for underwater attachment, and a change in the salt concentration is a possible trigger for this function in a marine biological adhesive. The peptide dissolved in water was confirmed to be of a monomeric form by GFC and MS. All of the cysteines were incorporated (i.e., with a free sulfhydryl group) in the chemical synthesis, and maintenance of a free sulfhydryl group in the solvent was confirmed by both an alkylation test and ESI-MS.

Table 2. Conditions for the Formation of a Meshlike Mesoscopic Structure

	peptide	preincubation[a]		salt treatment[a]	dialysis[a]	microstructure[b]
1	cMr20-S5	water		1 M NaCl/PBS	water	filament
2	cMr20-S5	water	O.N.	1 M NaCl/PBS	water	filament
3	cMr20-S5	NaPB (pH 6)	O.N.	1 M NaCl	NaPB (pH 6)	filament
4	cMr20-S5	NaPB (pH 8)	O.N.	1 M NaCl	NaPB (pH 8)	mesh
5	cMr20-S5	TrisB (pH 8)	O.N.	1 M NaCl	TrisB (pH 8)	mesh
6	cMr20-S5	NaPB (pH 8)	O.N.	1 M NaCl	NaPB (pH 6)	mesh
7	cMr20-S5	NaPB (pH 8)	3 h	1 M NaCl	NaPB (pH 8)	mesh
8	cMr20-S5	NaPB (pH 8)	3 h	1 M NaCl	NaPB (pH 6)	filament
9	cMr20-S5	NaPB (pH 8)	O.N.	1 M NaCl	NaPB (pH 8) to NaPB (pH 6)	mesh
10	cMr20-S5	NaPB (pH 6)	O.N.	1 M NaCl	NaPB (pH 8)	mesh
11	cMr20-S5	NaPB (pH 6)	O.N.	1 M NaCl	NaPB (pH 6) to NaPB (pH 8)	filament
12	cMr20-S5(Ser)	water		1 M NaCl/PBS	water	filament
13	cMr20-S5(Ser)	NaPB (pH 8)	O.N.	1 M NaCl	NaPB (pH 8)	filament

[a] The process used before AFM imaging comprised three subprocesses: preincubation, salt treatment, and dialysis. The salt treatment used was similar throughout the experiments, the peptide being incubated with 1 M NaCl for 10 min in each buffer solution. The buffer solutions used were 10 mM sodium phosphate (NaPB; pH 6 or pH 8) and 10 mM Tris-HCl (TrisB; pH 8). The period of preincubation was 3 h or overnight. "O.N." denotes overnight. [b] The mesoscopic structures of the self-assembled peptides are classified into "filament" or "mesh", being the "standard filament structure" typically formed in the self-assembly in 1 M NaCl/PBS, and the "meshlike structure" typically formed in the alkaline self-assembly, respectively.

DLS analysis, AFM imaging, and SEM visualization showed that the salt treatment at slightly acidic pH induced the peptide to self-assemble irreversibly. This self-assembly of the peptide may involve several types of mechanisms: intermolecular disulfide bond formation, noncovalent molecular interactions without disulfide bond formation, and a combination of both. To identify the mechanism for the self-assembly process, the peptide in which all cysteines had been substituted by serines, cMr20-S5(Ser), was chemically synthesized. The self-assembly behavior by the process at slightly acidic pH was nearly indistinguishable from that of the original peptide, cMr20-S5. This was also confirmed by the insensitivity of cMr20-S5 to the DTT treatment in the self-assembly. These results enabled us to conclude that the peptide had been self-assembled by noncovalent molecular interactions. Stability of the self-assembly against metal chelator (EDTA) treatment indicated that the molecular interactions are not simple salt bridges. The self-assembled peptides most studied so far have been a class of amphiphilic and/or β-structure type. In contrast, the peptides designed in this study did not fall into a simple class of amphiphilic or β-structure type. The peptides originating from Mrcp-20k belong to a new class of salt-dependent self-assembling peptides. Interestingly, initiation of the self-assembly process involved a threshold level of above 0.4 M NaCl. Since the original protein should express the function in seawater after being extruded from the cement duct,[3] the peptide may have inherited a threshold level close to the 0.55 M salt concentration of seawater. The visualization of peptide self-assembly by using various instruments showed that a macroscopic membrane had been formed by nanofilaments. No noticeable change in the CD spectrum after the salt treatment suggests that conformational change was not involved in the self-assembly process at slightly acidic pH. A charge-screening effect from salt could be suggested as the threshold mechanism for this self-assembly. However, it did not simply depend on the ionic strength and concentration of anions, because 0.5 M of divalent cationic salt did not trigger self-assembly, while 1 M of monovalent cationic salt did.

The pH dependence of the CD spectrum showed that the peptide conformation was changed at greater than pH 8. An unprecedented meshlike mesoscopic structure was found from visualization of the self-assembled peptide formed by the high-pH process. In this structure, nanofilaments were bundled into a fiber, whose formation made the boundary clear with an opening. A series of experiments was conducted to elucidate the formation process for the meshlike structure. The formation of this structure mostly depended on the alkaline pH range for preincubation or that for dialysis immediately after the salt treatment. DLS, ESI-MS, and GFC measurements showed the peptide, which had been incubated overnight at pH 8 to be monomeric with a different CD spectrum from that incubated at less than pH 7, with an increase in the positive band at 190−195 nm and a drastic decrease in the negative band at around 200 nm concomitant with a shift of the negative band toward a longer wavelength (Figure 3B). The resulting CD spectrum after incubation at pH 8−10 overnight is more similar to that of a β-sheet structure, which may suggest an increase in the ratio of β-structure at higher pH. While the alkaline salt treatment with dialysis at pH 6 gave the meshlike structure, a shorter than 3 h alkaline preincubation showed CD spectra close to those at less than pH 7 and gave a standard filament structure by the alkaline salt treatment with dialysis at pH 6. These results suggest that a long preincubation in the alkaline pH range induced the conformational change in the peptide molecule and was likely to be one of the essential factors for the formation of the meshlike structure. Whenever a standard filament structure was formed through salt treatment in the slight acidic pH range, sequential dialysis at alkaline pH affected the microscopic structure and resulted in a mesh. The conversion of a mesh from a standard filament may have been interpreted by further self-assembly of the monomeric molecules remaining in solution in addition to the microfilament self-assembly that had already been formed, since the initial phase of dialysis would have contained a substantial concentration of salt and may have provided appropriate conditions for alkaline self-assembly. This might also have provided the meshlike structural formation from the 3 h alkaline preincubation with alkaline dialysis. The sequential preincubation at pH 6 after pH 8 did not affect CD spectra of the peptide monomer. This indicated that the conformation at pH 8 is irreversible, being a possible reason that the mesh is the end-point mesoscopic structure.

The cysteines in the peptide samples are likely to have been the key factor in the pH-dependent conformational change that induced meshlike structural formation with the salt treatment. The CD spectra of the cysteine-free peptide, cMr20-S5(Ser), were almost the same at different pH values, including in the alkaline pH range. An alkylation test on cMr20-S5 indicated that a long alkaline preincubation affected the chemical form

of the cysteines and the formation of disulfide bonds. The combination of ESI-MS and GFC indicated the disulfide bonds are formed intramolecularly. The formation of a meshlike structure exclusively depended on the conformation of the monomer derived by intramolecular disulfide formation during the long alkaline preincubation. The alkaline pH value during the salt treatment may additionally have promoted the change of disulfide bonds into intermolecular links, although this effect was not examined in this study.

A complex biological system is generally formed through a molecular self-assembly process mainly with noncovalent interactions. Several findings on self-assembled peptides[10,26−28] have shown that self-assembly was encoded in the structure of proteins; therefore, learning from other extracellular protein systems has advantages to further design and fabrication of new materials. This study added a new biological adhesive to the list.

Acknowledgment. Thanks are given to Dr. Y. Matsuo, Mr. S. Matsuda, Dr. S. Kanai, Ms. M. Atsumi, Mr. Y. Urushida, and Dr. Y. Mori for their technical assistance. This work was performed as a part of The Industrial Science and Technology Project on Technological Development for Biomaterials Design Based on Self-Organizing Proteins that is supported by New Energy and Industrial Technology Development Organization.

Supporting Information Available. Atomic force microscopy and scanning electron microscopy observations of the cMr20-S5(Ser) self-assembly. This material is available free of charge via the Internet at http://pubs.acs.org.

References and Notes

(1) *Biological Adhesives*; Smith, A., Callow, J. Eds.; Springer-Verlag: Berlin and Heidelberg, Germany, 2006.
(2) Wösten, H. A. B. *Annu. Rev. Microbiol.* **2001**, *55*, 625−646.
(3) Kamino, K. In *Biological Adhesives*; Smith, A., Callow, J. Eds.; Springer-Verlag: Berlin and Heidelberg, Germany, 2006; pp 145−166.
(4) Waite, J. H.; Qin, X. X. *Biochemistry*. **2001**, *40*, 2887−2893.
(5) Waite, J. H. *Ann. N.Y. Acad. Sci.* **1999**, *875*, 301−309.
(6) Waite, J. H. *Int. J. Adhes. Adhes.* **1987**, *7*, 9−14.
(7) Rajagopal, K.; Schneider, J. P. *Curr. Opin. Struct. Biol.* **2004**, *14*, 480−486.
(8) Zhang, S. *Nat. Biotechnol.* **2003**, *21*, 1171−1178.
(9) Sarikaya, M.; Tamerler, C.; Jen, A. K.; Schulten, K.; Baneyx, F. *Nat. Mater.* **2003**, *2*, 577−585.
(10) Hyun, J.; Lee, W.-K.; Nath, N.; Chilkoti, A.; Zauscher, S. *J. Am. Chem. Soc.* **2004**, *126*, 7330−7335.
(11) Wright, E. R.; Conticello, V. P. *Adv. Drug Delivery Rev.* **2002**, *54*, 1057−1073.
(12) Huang, J.; Valluzzi, R.; Bini, E.; Vernaglia, B.; Kaplan, D. L. *J. Biol. Chem.* **2003**, *278*, 46117−46123.
(13) Aggeli, A.; Nyrkova, I. A.; Bell, M.; Harding, R.; Carrick, L.; McLeish, T. C. B.; Semenov, A. N.; Boden, N. *Proc. Natl. Acad. Sci. U.S.A.* **2001**, *98*, 11857−11862.
(14) West, M. W.; Wang, W.; Patterson, J.; Mancias, J. D.; Beasley, J. R.; Hecht, M. H. *Proc. Natl. Acad. Sci. U.S.A.* **1999**, *96*, 11211−11216.
(15) Silva, G. A.; Czeisler, C.; Niece, K. L.; Beniash, E.; Harrington, D. A.; Kessler, J. A.; Stupp, S. I. *Science.* **2004**, *303*, 1352−1355.
(16) Lashuel, H. A.; LaBrenz, S. R.; Woo, L.; Serpell, L. C.; Kelly, J. W. *J. Am. Chem. Soc.* **2000**, *122*, 5262−5277.
(17) Nowak, A. P.; Breedveld, V.; Pakstis, L.; Ozbas, B.; Pine, D. J.; Pochan, D.; Deming, T. J. *Nature* **2002**, *417*, 424−428.
(18) Nilsson, K. P. R.; Rydberg, J.; Baltzer, L.; Inganäs, O. *Proc. Natl. Acad. Sci. U.S.A.* **2003**, *100*, 10170−10174.
(19) Fernandez-Lopez, S.; Kim, H.-S.; Choi, E. C.; Delgado, M.; Granja, J. R.; Khasanov, A.; Kraehenbuehl, K.; Long, G.; Weinberger, D. A.; Wilcoxen, K. M.; Ghadiri, M.R. *Nature.* **2001**, *412*, 452−455.
(20) Deming, T. J. *Curr. Opin. Chem. Biol.* **1999**, *3*, 100−105.
(21) Dalsin, J. L.; Hu, B.-H.; Lee, B. P.; Messersmith, P. B. *J. Am. Chem. Soc.* **2003**, *125*, 4253−4258.
(22) Kamino, K. *Biochem. J.* **2001**, *356*, 503−507.
(23) Holmes, T. C.; de Lacalle, S.; Su, X.; Liu, G.; Rich, A.; Zhang, S. *Proc. Natl. Acad. Sci. U.S.A.* **2000**, *97*, 6728−6733.
(24) Sakaguchi, K.; Fukase, M.; Kobayashi, I.; Kimura, T.; Sakakibara, S.; Katsuragi, S.; Morita, K.; Noda, T.; Fujita, T. *J. Bone Miner. Res.* **1987**, *2*, 83−90.
(25) Azriel, R.; Gazit, E. *J. Biol. Chem.* **2001**, *276*, 34156−34161.
(26) Zhang, S.; Holmes, T.; Lockshin, C.; Rich, A. *Proc. Natl. Acad. Sci. U.S.A.* **1993**, *90*, 3334−3338.
(27) Jin, H. J.; Kaplan, D. L. *Nature* **2003**, *424*, 1057−1061.
(28) Gazit, E. *FEBS J.* **2005**, *272*, 5971−5978.

BM0612236